

An Interdisciplinary Agent-based Evacuation Model: Integrating Natural Environment, Built environment, and Social System for Community Preparedness and Resilience

Chen Chen^{*1}, Charles Koll², Haizhong Wang³, Michael K. Lindell⁴

^{*1}Corresponding Author: College of Engineering, Architecture, and Technology, Oklahoma State University, Stillwater, OK, 74078.

²School of Electrical Engineering and Computer Science, Oregon State University, Corvallis, OR 97331.

³ School of Civil and Construction Engineering, Oregon State University, Corvallis, OR 97331.

⁴Department of Urban Design and Planning, University of Washington, Seattle, WA 98195.

Correspondence to: Chen Chen (chen.chen10@okstate.edu)

Abstract: Previous tsunami evacuation simulations have mostly been based on arbitrary assumptions or inputs adapted from non-emergency situations, but a few studies have used empirical behavior data. This study bridges this gap by integrating empirical decision data from local evacuation expectations surveys and evacuation drills into an agent-based model of evacuation behavior for two Cascadia Subduction Zone (CSZ) communities that would be inundated within 20-40 min after a CSZ earthquake. The model also considers the impacts of liquefaction and landslides from the earthquake on tsunami evacuation. Furthermore, we integrate the slope-speed component from Least-cost-distance to build the simulation model that better represents the complex nature of evacuations. The simulation results indicate that milling time and evacuation participation rate have significant non-linear impacts on tsunami mortality estimates. When people walk faster than 1 m/s, evacuation by foot is more effective because it avoids traffic congestion when driving. We also find that evacuation results are more sensitive to walking speed, milling time, evacuation participation, and choosing the closest safe location than to other behavioral variables. Minimum tsunami mortality results from maximizing the evacuation participation rate, minimizing milling time, and choosing the closest safe destination outside of the inundation zone. This study's comparison of the agent-based model and the Beat-the-Wave (BtW) model finds consistency between the two models' results. By integrating the natural system, built environment, and social system, this interdisciplinary model incorporates substantial aspects of the real world into the multi-hazard agent-based platform. This model provides a unique opportunity for local authorities to prioritize their resources for hazard education, community disaster preparedness, and resilience plans.

39 1. Introduction

40 Recent devastating earthquakes and tsunamis have placed immense burdens on their affected
 41 communities, such as the 2011 Tohoku tsunami (Mori et al., 2011), the 2009 American Samoa
 42 tsunami (Lindell et al., 2015), and the 2018 Indonesia Sulawesi tsunami (Sassa and Takagawa,
 43 2019). Due to a small evacuation time window between the end of earthquake shaking
 44 and the arrival of the first tsunami wave, a high level of evacuation efficiency is essential
 45 for minimizing the loss of life in low-lying coastal communities subject to local tsunamis
 46 (Wang et al., 2016; Raskin and Wang, 2017). To reduce evacuation clearance time (the
 47 sum of authorities’ decision time, warning dissemination time, households’ preparation time,
 48 and evacuation travel time) and thus maximize survival rates during tsunamis, researchers
 49 and practitioners have developed evacuation simulations to support decision-making, public
 50 education, and community emergency planning and management.

51 1.1. Previous ABMSs for Earthquake and Tsunami Evacuation

52 Agent-based modeling and simulation (ABMS), as a type of highly effective computational
 53 simulation model, has been applied to many research fields (Mas et al., 2013; Mostafizi
 54 et al., 2019a). The unique characteristics of ABMS include a bottom-up structure and
 55 ability to model heterogeneous agents and their interactions with other agents. These unique
 56 characteristics meet the needs of disaster evacuation simulation (Gilbert, 2007). The bottom-
 57 up structure provides an opportunity to analyze how changes in evacuation behavior affect
 58 the overall evacuation result. One concern about using ABMS is the computational expense,
 59 but this is less of an issue as computing costs continue to decrease (Lindell et al., 2019).
 60 This increase in computational power has allowed disaster researchers to apply ABMS to
 61 1) simulate evacuation in large-scale communities and 2) integrate different layers of data
 62 to comprehensively analyze evacuation with consideration of interactions between the nat-
 63 ural environment, built environment, and social system. Table 1 identifies recent tsunami
 64 evacuation ABMS studies and their content.

Table 1: Recent earthquake and tsunami ABMS studies

Author / Year	Study Area	Mode	Model Components			Tested Variables
			Natural Environment	Built Environment	Social System	
Chen and Zhan (2008)	San Marcos, TX, USA	Car	N/A	Road network; artificial safe zone	Hypothetical population density; dynamic routing; car following model	Evacuation strategy
Dawson et al. (2011)	Towyn, United Kingdom	Car	Flood inundation	Road network; destination; building	Population distribution; warning time; driving speed; re-route	Warning time; water depth
Karon and Yeh (2011)	Cannon Beach, OR, USA	Walk	Tsunami inundation	Road network; destinations	Warning dissemination; shortest distance; travel speed	Infrastructure retrofitting strategy
Mas et al. (2012)	Arahama village, Japan	Car/Walk	Tsunami inundation	Road network; destinations	Population distribution; evacuation mode; milling time; speed	Evacuation result compared with real event; milling time; destination
Mas et al. (2013)	La Punta, Peru	Car/Walk	Tsunami inundation	Road network; destinations	Population distribution; social status; evacuation mode; milling time; speed	Evacuation result; shelter capacity
Wang et al. (2016)	Seaside, OR, USA	Car/Walk	Tsunami inundation	Road network; destinations	Population distribution; milling time; evacuation mode; speed; route choice	Water depth; milling time; evacuation mode; destination location
Mostafizi et al. (2019a)	Seaside, OR, USA	Walk	Tsunami inundation	Road network; destinations	Population distribution; milling time; speed	Shelter location

65 In the absence of empirical behavioral data, early-stage evacuation ABMSs were based on
 66 arbitrary assumptions, as had been the case for large-scale evacuation models (Lindell and
 67 Perry, 1992; Lindell and Prater, 2007). Chen and Zhan (2008) investigated the effectiveness
 68 of simultaneous and staged evacuation strategies using an ABMS for San Marcos, Texas.
 69 Although this study considered evacuees’ car following and dynamic routing behaviors, it
 70 was based on many arbitrary assumptions about evacuation behavior, such as homogeneous
 71 milling time within a zone, single evacuation mode, evacuees selecting quickest evacuation

72 route and destination, etc. To reduce reliance on assumptions, Mas et al. (2012) built
73 an evacuation ABMS that included more empirical data from the natural system, built
74 environment, and social system. In this model, agents are characterized by probabilistic
75 distributions of milling time, evacuation mode choice, evacuation destination, and travel
76 speed. By comparing the simulation with data from the 2011 Japanese earthquake and
77 tsunami, the authors concluded that the results from this simulation are consistent with the
78 real event and can be used to analyze evacuation and shelter demand for future events. In
79 2013, Mas et al. (2013) expanded this ABMS to the city of La Punta, Peru to conduct a
80 vertical and horizontal shelter analysis.

81 Practitioners and researchers have relied on similarities between the 2011 Japanese earth-
82 quake event and the geologically similar Cascadia Subduction Zone (CSZ) to encourage
83 Oregon coastal residents to prepare for local tsunamis. Karon and Yeh (2011) used GIS to
84 build an evacuation ABMS by integrating tsunami inundation, warning transmission, and
85 travel speed to examine the impact of failures of critical infrastructure in Cannon Beach,
86 Oregon. To model heterogeneous agent behaviors, Wang et al. (2016) established a scenario-
87 based tsunami evacuation ABMS for Seaside, Oregon. This study examined the impact of
88 variance in agent behaviors such as milling time, evacuation mode choice, and travel speed.
89 In addition, it also included the impact of a tsunami, but not an earthquake, on the built
90 environment such as damage to streets, bridges, and buildings. A later version of this study,
91 Mostafizi et al. (2019a), used a similar ABMS platform to identify optimum shelter loca-
92 tions considering the population distribution, heterogeneous agent milling time, and walking
93 speed. However, as with previous studies, agents were assumed to evacuate to the closest
94 shelter, which may not accurately represent people’s destination choices when threatened by
95 a tsunami.

96 One common limitation of those evacuation models is that they have evacuation assumptions
97 about the four evacuation time components – authorities’ decision delay time, households’
98 warning receipt and decision time, households’ evacuation preparation time, and households’
99 evacuation travel time. Warning receipt time, for example, can vary across communities
100 and households. Nagarajan et al. (2012) used an ABMS to test the warning dissemination
101 speed through formal channels transmitted by officials and informal channels transmitted
102 by neighbors. They found that even a small proportion of people who were willing to warn
103 their neighbors has a considerable impact on reducing warning dissemination time. Several
104 previous ABMS studies have also assumed arbitrary probability functions for milling time
105 to represent the variance in evacuation departure times (Mas et al., 2012; Wang et al., 2016;
106 Mostafizi et al., 2019a).

107 In addition, some recent evacuation simulations have also employed assumptions about the
108 distribution of evacuees’ walking speeds. For instance, Wang et al. (2016) and Mostafizi
109 et al. (2019a) assumed a normal distribution of evacuee walking speeds for which the mean
110 was built based on a study of pedestrians walking on streets in non-emergency situations
111 (Knoblauch et al., 1996). This assumption is likely to underestimate travel speeds in a
112 tsunami evacuation and thus overestimate tsunami mortality rates. However, mortality
113 rates might not be overestimated if travel speed is actually reduced by additional barriers
114 such as landslides, liquefaction, and other earthquake disturbances to the evacuation route
115 system.

116 Failure to consider “shadow evacuation” by residents of areas outside the tsunami inundation

117 zone can lead to unnecessary evacuation that overwhelms the evacuation route system and
118 impedes travel by people in the inundation zone (Lindell et al., 2019). Instead of assigning a
119 probabilistic distribution to walking speed, Wood and Schmidlein (2012) used a determin-
120 istic hiking function (Tobler, 1993) to define a least cost distance (LCD) model for tsunami
121 evacuation. This hiking function captured the impact of slope on walking speed, but also
122 assumed daily walking conditions rather than emergency conditions. Overall, existing evac-
123 uation models have assumed that pedestrians’ travel behavior in daily situations represents
124 the corresponding behavior in evacuations, but field or experimental data to confirm this
125 assumption are needed.

126 Most of the aforementioned studies used Census data to identify agents’ evacuation departure
127 locations, so the scenarios assumed people were at home. However, a disaster may happen at
128 any time of the day. To account for the variance in evacuees’ locations, Dawson et al. (2011)
129 developed a flood management ABMS to support flood emergency planning and evaluate
130 flood incident management measures. The authors used empirical survey data to integrate
131 warning time and used the National Travel Survey to determine people’s locations and travel
132 states (e.g., work, home, or school).

133 *1.2. Other Models for Earthquake and Tsunami Evacuation*

134 Although scenario-based ABMSs have been employed to support evacuation decision-making
135 for entire communities (or large areas), jurisdictions are also interested in the question of how
136 quickly people should evacuate from different sub-areas in a community. Geographers used
137 the LCD method to build the Beat-the-Wave (BtW) model to estimate the maximum travel
138 time that people need to walk out of a tsunami inundation zone (Wood and Schmidlein,
139 2012). This model defined the distance cost by two variables – the evacuation route’s slope
140 and its land cover. To determine the walking speed, they employed Tobler’s hiking function
141 (Tobler, 1993) and the energy cost of the terrain category (Soule and Goldman, 1972). The
142 output of this model provides the spatial distributions of maximum evacuation times to
143 “beat the wave”, and can be used for preparedness planning and education. The Oregon
144 Department of Geology and Mineral Industries (DOGAMI) has implemented this model
145 to identify Oregon coastal communities’ evacuation route maps and to estimate evacuation
146 travel times (DOGAMI, 2020; Gabel et al., 2019).

147 Although DOGAMI has used the LCD method because it is relatively easy to calculate and
148 provides reasonable evacuation time estimates (ETEs), it does have some limitations. First,
149 it cannot examine social system variables that influence tsunami evacuation outcomes (such
150 as population distribution, milling time, and the choice of transportation mode, evacuation
151 route, and evacuation destination). Second, it cannot incorporate dynamic travel costs due
152 to crowding or congestion. Agent-based models can overcome those limitations but are
153 sometimes criticized as difficult to implement due to the magnitude of data required. As
154 noted earlier, those data include the distribution of population locations, evacuees’ behaviors,
155 and wave-arrival time. However, the ABMS and LCD approaches are not incompatible so
156 a mixed-method approach could be used to better model the complex nature of evacuation
157 (Wood and Schmidlein, 2012).

1.3. Research Objectives and Questions

The preceding literature review has revealed the need for an evacuation ABMS that can simultaneously consider the natural environment, built environment, and social system to analyze complex evacuation scenarios. Although some studies have incorporated layers from those three systems, most of the data inputs were arbitrary assumptions – a problem that has plagued large scale evacuation modeling (Lindell et al., 2019). To more completely integrate the three systems, this study established an ABMS for tsunami evacuation that integrates 1) the natural environment and its disruptions; 2) the built environment and its disruptions; and 3) the social system, as defined by people’s protective actions – especially their evacuation behavior.

Specifically, this ABMS integrates human decisions and evacuation logistics into an ABMS platform using empirical behavior data that were collected through survey questionnaires and evacuation drills from coastal residents facing tsunami threats. This integration operationalizes the Protective Action Decision Model (PADM) (Lindell and Perry, 2012) within an ABMS by incorporating agents’ heterogeneous behavior in emergencies, such as 1) evacuation participation; 2) choices of transportation mode, evacuation routes and destinations; and 3) travel speeds. Furthermore, to accurately model the complex nature of evacuation, this ABMS also includes the impact of landslides and liquefaction on the road network during evacuation. Incorporating the essential components of the LCD model (slope and road surface) combines the advantages of the ABMS and BtW models (Wood and Schmidlein, 2012). ABMS models are implemented for Coos Bay, Oregon and sensitivity analyses are conducted in this study to answer the following questions:

1. How do the evacuation participation rate, milling time, mode choice, destination choice, and travel speed affect mortality rates?
2. Which of these variables have greater impact on mortality rates and which of them can be addressed in tsunami evacuation preparedness?
3. How do the results from the ABMS compare with the results from the BtW model?

This interdisciplinary ABMS can not only serve as an evacuation planning tool for local agencies, but also can be an educational and assessment tool for coastal residents to better prepare for the next threat.

2. Interdisciplinary Tsunami Evacuation ABMS

2.1. Agent-based Modeling Environment

Simulating evacuation is a computationally-intensive problem due to the large scale of the built and natural environments and the complexity of agent behaviors. Therefore, an ABMS typically has a high computational cost when applied to large scale evacuation (Lindell et al., 2019). To overcome this issue, the tsunami evacuation ABMS was built using the Julia programming language, which is a just-in-time compiled language, allowing for high performance and computational speed (Bezanson et al., 2012). The high speed of the Julia language allows researchers to model large communities with detailed heterogeneous agent behaviors. This study’s ABMS modeling environment allows users to modify parameters for natural, built, and social systems and also allows stochastic inputs. Figure 1 shows the ABMS visualization and real-time evacuation monitors. The details of the evacuation model environment are discussed in Section 2.3.

201 *2.2. Study Area*

202 A series of CSZ tsunami evacuation studies have used Seaside, OR as a study community
 203 because of its high level of vulnerability to local tsunamis (Connor, 2005; Wood et al., 2015;
 204 Wang et al., 2016; Chen et al., 2020, 2021). However, other communities that differ from
 205 Seaside in their geographic and demographic characteristics should also be examined. This
 206 study chose the Coos Bay peninsula as a case study due to four features. First, it has a
 207 distinctly vulnerable geography. As Figure 1 indicates, this peninsula is surrounded by bay
 208 water on its north, east, and west sides. In addition, its hilly spine in the middle provides
 209 ready access to higher ground for evacuation destinations. The bay serves as the second
 210 and the sixth largest estuary in Oregon and on the US west coast, respectively (CLW,
 211 2015). Second, this community is located on the southern margin of the CSZ, where the
 212 rupture probability is higher and tsunami wave arrival time is shorter than communities
 213 farther north (Priest et al., 2014; Chen et al., 2021). Third, the Coos Bay peninsula has
 214 a total population of about 26,129, which is the largest population among Oregon coastal
 215 communities (United State Census Bureau, 2020). Moreover, a large proportion of the
 216 population (about 25%) resides within the inundation zone. Fourth, this community has a
 217 high level of social vulnerability due to its demographic characteristics. The local population
 218 has a higher percentage of disabled residents and is poorer and less educated than the overall
 219 U.S. population (United State Census Bureau, 2020; Chen et al., 2021).

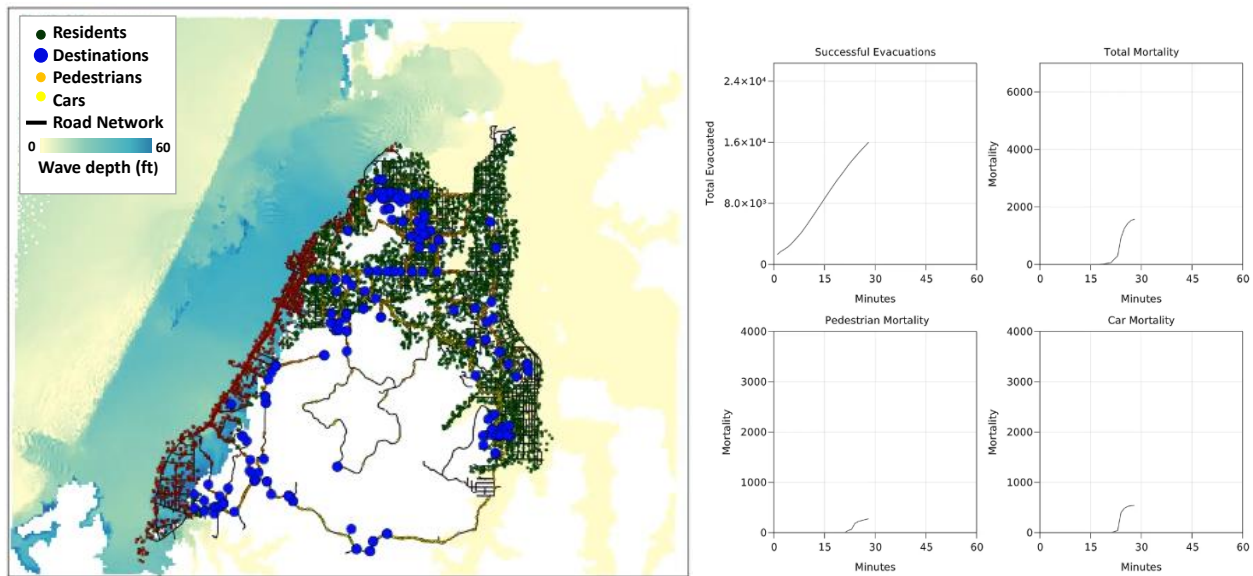


Figure 1: Simulation model visualization of Coos Bay, Oregon

220 *2.3. Model Components*

221 To more accurately model tsunami evacuation, this study proposes an ABMS that integrates
 222 components of the natural environment, built environment, and social system. Specifically,
 223 this ABMS includes the components shown in Table 2.

Table 2: ABMS components

System	Component	Description	Data sources
Natural environment	Tsunami inundation layer	Water depth per 30 sec time frame (m)	DOGAMI CSZ near-filed M9 XXL scenario
	Elevation and slope	Use elevation digital model to calculate slope	Oregon 10m Digital Elevation Model (DEM)
	Landslide and liquefaction	Landslide and liquefaction susceptibility to identify disrupted roads	DOGAMI Project O-13-06
Built environment	Road Network	Links	OpenStreetMap & Google Earth
	Non-retrofitted bridges	Manually identified by talking with local authorities	DOGAMI Project O-19-07
Social System	Population distribution	26,000 agents US Census by census block group, then randomly generate along transportation network	US Census
	Evacuation participation	By attributes or proportion (1: evacuate; 0: stay)	Survey
	Milling time	Gamma distributions and a fixed time	Survey
	Mode choice	Proportion, controlled by a parameter	Survey
	Destination choice	Probability distribution on the distance to shelter and use soft-max function to calculate the discrete probability	Survey: distance from home to destination separated by car/foot, gamma distribution
	Evacuation speed – car	IDM model with parameters and a speed limit	Parameter chosen by common scenarios
	Evacuation speed – foot	Evacuation hiking function based on elevation	Evacuation drills
	Route choice	Shortest distance to the destination that agents chose	
Route diversion	If next intersection is blocked, the agent selects another leg of the intersection, then chooses another destination		

224 *2.3.1. Social System and Agent Behavior*

225 According to the PADM, people make protective action decisions based on environmen-
 226 tal/social cues and warnings, which are affected by personal characteristics such as pre-
 227 existing beliefs about the hazard, protective actions, and community stakeholders (Lindell
 228 and Perry, 2012; Lindell, 2018). The large number of these variables, the difficulty in mea-
 229 suring them, and their heterogeneity among agents makes it difficult to model this part of the
 230 evacuation process (Mas et al., 2012). Previous evacuation simulation models (Mas et al.,
 231 2012; Wang et al., 2016; Mostafizi et al., 2017, 2019b) assumed that residents evacuate in the
 232 most efficient manner (such as selecting the closest shelter), but ignored the heterogeneity
 233 in evacuation decisions and actions (Gwynne et al., 1999). One main reason is that these
 234 models lacked empirical data on evacuation decisions and actions. To fill that gap, the evac-
 235 uation model in this study integrates data on people’s evacuation decisions and actions that
 236 were collected from questionnaire surveys and evacuation drills.

237 This study employed the PADM as the framework for a mail-based household question-
 238 naire survey that collected data on household evacuation intentions in the Coos Bay area
 239 between May and September 2020. There were 258 respondents who returned the ques-
 240 tionnaire, which covers their evacuation intentions, expected milling process, and choices of
 241 transportation modes and destinations, as well as psychological variables and demographic
 242 characteristics. More information can be found in Chen et al. (2021). Probability distribu-
 243 tions on these variables are utilized to model the heterogeneous evacuation actions from the
 244 data shown in Table 2.

245 The analyses that follow are based on the ETE model in which the time to clear the risk area
 246 is a function of authorities’ decision time, warning dissemination time, evacuation prepara-
 247 tion time, and evacuation travel time (Lindell et al., 2019). Evacuation preparation time,
 248 which is often called “milling” (Wood et al., 2018), has two components – 1) psychological
 249 preparation, which involves information seeking and processing to make evacuation decisions;
 250 and 2) logistical preparation, which involves performing essential tasks (e.g., packing bags
 251 and securing the home) before leaving (Lindell and Perry, 2012). Evacuation travel time
 252 is a function of evacuees’ choices of transportation mode, evacuation route, and evacuation
 253 destination.

254 Modeling evacuation from a distant tsunami requires data on authorities’ decision time and
 255 warning receipt time. In the absence of these data, the results of the following analyses

do not apply to distant tsunamis. Modeling evacuation from a local tsunami is simpler because long and strong earthquake shaking is a reliable environmental cue to tsunami onset. Consequently, people who recognize this environmental cue have authorities’ decision time and warning dissemination time equal to zero.

Moreover, the following analyses include sensitivity analyses that examine the impact of a plausible range of variation in the input variables on the estimated tsunami mortality rate. As discussed below, these sensitivity analyses can provide useful information for decision making and emergency planning.

Evacuation participation (0: stay; 1: leave) is the protective action that an individual agent selects in response to earthquake shaking or a tsunami warning in this model. According to the Coos Bay community survey, 81% of the respondents intend to evacuate, regardless of their location inside (“compliant evacuees”) or outside (“shadow evacuees”) of the tsunami inundation zone. Thus, 81% is used as the evacuation participation rate in this model, with a sensitivity analysis on how a change in this rate would impact tsunami mortalities. Evacuees’ origins are determined by their locations when an earthquake occurs or a tsunami warning is received. Thus, there is spatial and temporal variability in the distribution of population locations based on factors such as time of day, season, and weather (Wang et al., 2016). This study utilized 2020 US Census (United State Census Bureau, 2020) data to define the origins of 26,363 agents. The scenario examined in this study assumes that all residents are at home, as on a weekend or at night.

The tsunami evacuation intentions questionnaire asked respondents to report how much time they expected it would take them to prepare to evacuate. As shown in equation 1,

$$f(x; \alpha, \beta) = \frac{\beta^\alpha x^{\alpha-1} e^{-\beta x}}{\Gamma(\alpha)} \quad \text{for } x > 0 \quad \alpha, \beta > 0 \quad (1)$$

where x means the milling time and $f(x)$ means the probability of having that milling time for an individual. Applying maximum likelihood estimation to the survey data produced $\alpha = 1.659$ and $\beta = 6.494$ as the estimated parameters of the gamma function for the **milling time** distribution. As Figure 2 indicates, both the Weibull and lognormal distributions provided poorer fits (AIC and BIC) to the data.

Transportation mode choice is a critical factor that affects evacuation success. Agents can choose to evacuate either by foot or by personal vehicle in this model (0: car; 1: foot). In Coos Bay, 70% of the survey respondents reported that they would evacuate by car and only 27% expected to evacuate by foot (Chen et al., 2021).

Destination choice is also obtained from the survey and a probability of choosing a specific destination is assigned to each evacuee based on their distance from the available destinations. A gamma function yields the best goodness-of-fit statistics among the three candidate functions for the destination selection probability, shown in Figure 3. Probability functions were developed separately for evacuation by foot and by car, with maximum likelihood estimation yielding $\alpha = 1.920$ and $\beta = 500$ for evacuation by foot and $\alpha = 1.646$ and $\beta = 1.745$ for evacuation by car.

After agents choose their expected evacuation destinations, the model assigns them to the **shortest route** that is calculated by the A* algorithm (Hart et al., 1968) on the road network. To simulate the behavior of people who encounter an evacuation impediment such as flood on the road while evacuating, agents **divert** to an alternate route. Specifically, when

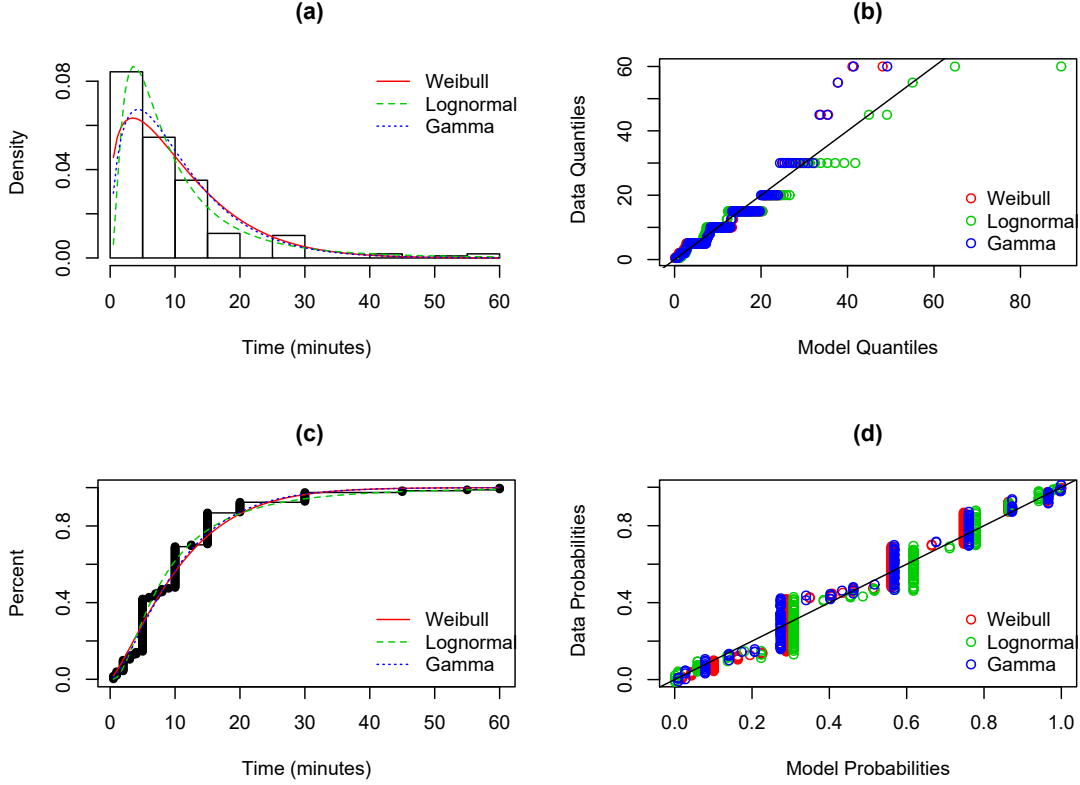


Figure 2: Expected preparation time from survey data and fitted models: (a) data histogram and probability density function; (b) Quantiles-Quantiles plot; (c) cumulative density function; (d) Probabilities-Probabilities plot.

298 agents observe that the next intersection is (inundated by water or damaged by hazards i.e.
 299 see section 2.3.3), they select a different leg of the intersection. The model assumes an equal
 300 probability of choosing each of the unblocked legs.

301 The mechanism for assigning a **travel speed** varies, depending on which transportation
 302 mode an agent chooses (foot or car). Driving speed is determined by the IDM car following
 303 model (Treiber et al., 2000) and the vehicle speed limit on that roadway. Pedestrian walking
 304 speed is determined by the slope of the ground on which the pedestrians are walking, through
 305 an advanced Hiking Function (Tobler, 1993; Wood and Schmidlein, 2012). To adjust for
 306 differences in walking speeds between daily walking and a tsunami evacuation, we modified
 307 the hiking function based on tsunami evacuation drill data that were collected from 2016-
 308 2018 (Cramer et al., 2018). In these evacuation drills, 136 evacuees' trajectory data (source:
 309 author) were recorded by GNSS embedded mobile devices. The walking speed and slope
 310 data were used to modify the hiking function; the modified function is shown in Equation 2.

$$Speed = 1.65 \times e^{(-2.30 \times \text{abs}(Slope - 0.004))} \quad (2)$$

311 To reduce computational cost and optimize simulation speed, the model assigns an average
 312 slope to the road segment between each pair of intersections and agents who walk on that
 313 segment will have the walking speed that is determined by Equation 2. When conduct-

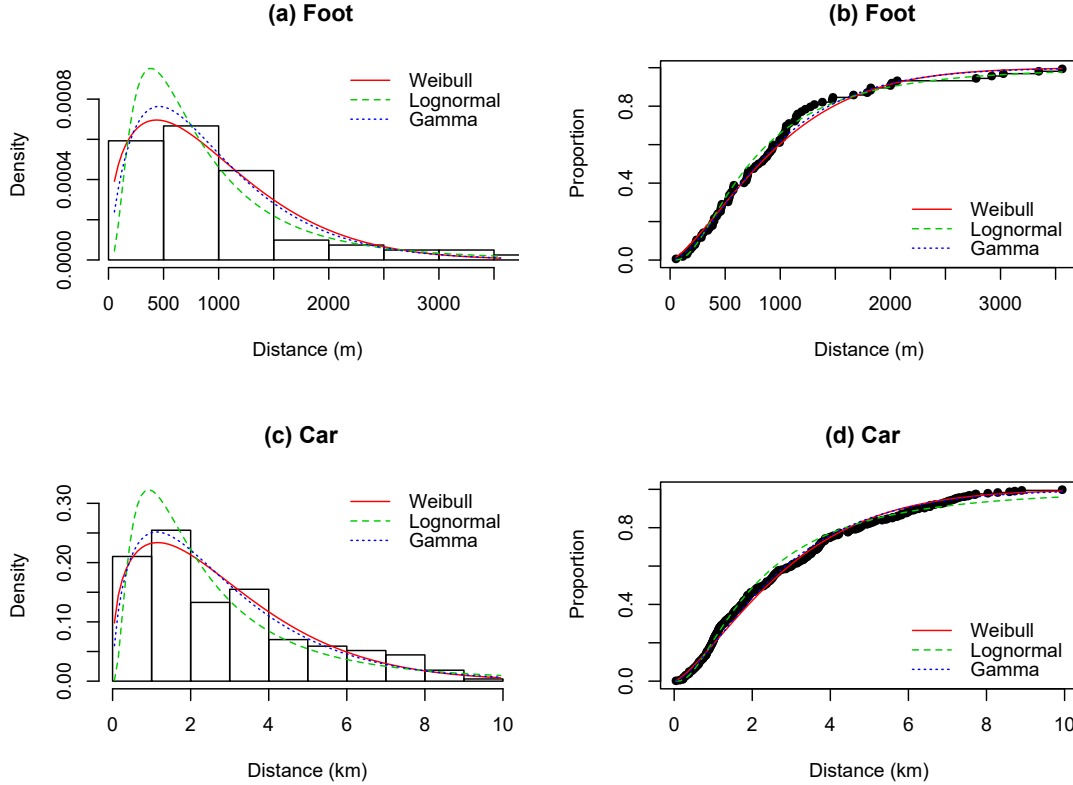


Figure 3: Intended evacuation destination from survey data and fitted models. Panels (a) and (c) are probability density functions; panels (b) and (d) are cumulative distribution functions.

314 ing sensitivity analyses for different values of walking speed, the modified hiking function
 315 is disabled when a fixed walking speed is used. Moreover, pedestrian walking speed is re-
 316 duced based on the conservative value when liquefaction and landslide block a road surface
 317 (Schmidlein and Wood, 2015; Gabel et al., 2019). More details are discussed in Section
 318 2.3.3.

319 2.3.2. Built Environment

320 The model’s built environment components include the road network and non-retrofitted
 321 bridges. The transportation network was obtained from OpenStreetMap (OSM, 2021) and
 322 updated manually by the authors based on the 2020 Google Earth satellite image (Google,
 323 2021). All roads are considered to be two-way one-lane streets, as a conservative assumption
 324 (Wang et al., 2016). This model also assumes that all agents, whether as pedestrians or in
 325 cars, follow the road network to their destinations. Alternative evacuation routes are not
 326 included in this simulation, such as swimming across streams or cutting through open fields
 327 or parking lots.

328 Non-retrofitted bridges were located using a study by (Gabel et al., 2019). These bridges
 329 are not expected to survive after an M9 CSZ earthquake (Gabel et al., 2019), so they are
 330 assumed to be undrivable and unwalkable in this analysis. These bridges are:

- 331 • Virginia Ave. on Pony Creek, (1) in Figure 4

- 332 • Vermont Ave. on Pony Creek, (2) in Figure 4
- 333 • Broadway Ave. on Pony Creek, (3) in Figure 4

334 2.3.3. *Natural environment*

335 Natural Environment components that are integrated in this model include tsunami inun-
336 dation, terrain elevation and slope, liquefaction susceptibility, and landslide susceptibility.

337 **Tsunami inundation layer:** This model simulates an M9 CSZ earthquake and tsunami
338 using the XXL tsunami inundation model (Witter et al., 2011; Priest et al., 2013). The
339 tsunami inundation layer includes variation in the flow depth and velocity every 30 seconds
340 for each 15-m grid cell from the time the tsunami is generated to eight hours after it reaches
341 the Coos Bay peninsula. The inundation model assumes “bare earth”, so the impact of large
342 buildings on water flow was not included.

343 **Topographical elevation and slope:** A 10-m digital elevation model created by U.S.
344 Geological Survey (USGS) (Oregon Geospatial Enterprise Office, 2017) is included as the
345 surface topographical elevation data. In this simulation, elevation data is utilized to calculate
346 the surface slope to inform agents’ walking speed using the modified hiking function shown in
347 Equation 2. The slope is calculated by using elevation change (Δy) divided by the Euclidean
348 distance (Δx) change between two points, expressed as ($\text{Slope} = \Delta y / \Delta x$).

349 **Landslides and liquefaction:** Evacuation routes can become undrivable and even unwalk-
350 able due to liquefaction, rockfalls, and lateral spreading (Gabel et al., 2019). Susceptibility
351 to both landslide and liquefaction for Coos Bay (Franczyk et al., 2019) is included in this
352 model to estimate which road segments will be disrupted.

353 Landslide susceptibility is calculated based on proximity to landslide deposits, susceptible
354 geologic units, slope angles, and existing landslide inventory. Areas are classified into four
355 susceptibility levels – low, moderate, high, and very high (Burns et al., 2016; Franczyk et al.,
356 2019). Liquefaction susceptibility is calculated from the cohesionless sediments, based on
357 Youd and Perkins (1978); Madin and Burns (2013). Areas are classified into five susceptibility
358 levels – very low, low, moderate, high, and very high. This produces conservative liquefaction
359 levels because it assumes relatively shallow groundwater (Madin and Burns, 2013).

360 Table 3 shows the landslide and liquefaction susceptibility levels that are used in this simu-
361 lation. The spatial areas having a moderate or higher susceptibility level of either landslide
362 or liquefaction are assumed to be disrupted after an M9.0 CSZ earthquake. We consider the
363 moderate level as a threshold to be conservative and realistic. This threshold also has been
364 used by local authorities (Gabel et al., 2019) to build the Coos Bay BtW model. As shown
365 in Figure 4, 54% of the transportation network is exposed to at least a moderate level of
366 liquefaction-landslide susceptibility and 21% is exposed to at least a high level. Thus, the
367 transportation network is likely to be significantly disrupted after an M9.0 earthquake.

368 In this simulation, a street that is predicted to be disrupted by landslide or liquefaction
369 is assigned a rocky or muddy road surface that prevents evacuees from driving through the
370 impediment and makes walking the only feasible transportation mode from that point. Wood
371 and Schmidtlein (2012) adapted a speed conservation value from Soule and Goldman (1972),
372 which is applied to the travel speed of people walking on muddy or rocky terrain surfaces.
373 These values are shown in Table 4.

Table 3: Landslide and liquefaction susceptibility for network disruption in ABMS

		Landslide Susceptibility			
		Low (0)	Moderate (1)	High (1)	Very high (1)
Liquefaction Susceptibility	Very low (0)	0	1	1	1
	Low (0)	0	1	1	1
	Moderate (1)	1	1	1	1
	High (1)	1	1	1	1
	Very high (1)	1	1	1	1

Using a disjunctive decision rule, a spatial area with an index value of at least moderate (54%) or high (21%) level is assumed to be disrupted after an M9 earthquake

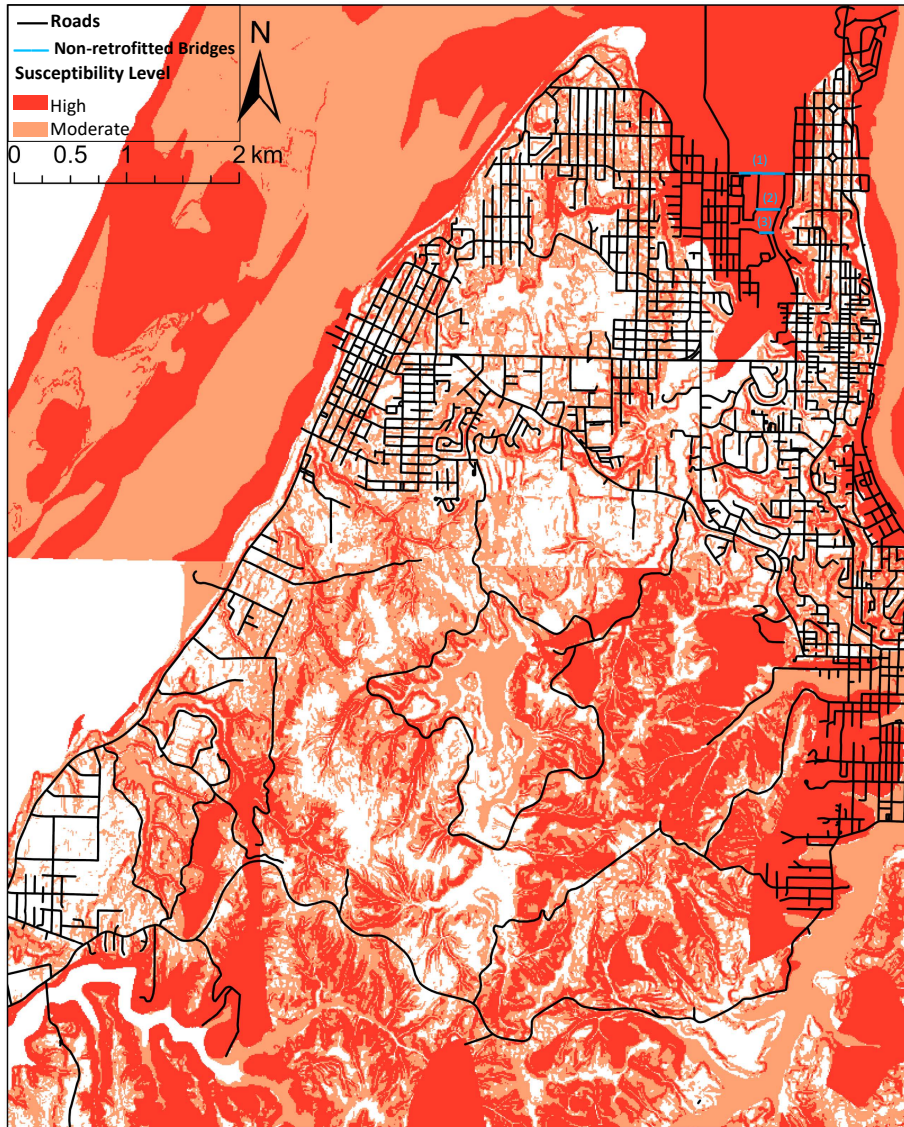


Figure 4: Coos Bay landslide and liquefaction susceptibility

Table 4: Speed conservation values used in modeling pedestrian walking speed (Wood and Schmidlein, 2012)

Feature Type	Speed Conservation Value
Road (Paved)	1
Unpaved Trails	0.9091
Dune Trails (Packed Sand)	0.5556
Muddy Bog	0.5556
Beach (Loose Sand)	0.476

Speed conservation values adapted from Soule and Goldman (1972)

374 **3. Results and Discussion**

375 Figure 5 shows the overall visualization of one run of the model from 0 – 60 mins after the
 376 M9 earthquake. The model assumes that 1) the deformation of subduction zone completes
 377 and tsunami is triggered at the source when $t = 0$ mins; 2) people start the milling process
 378 and evacuate either by foot or car; and 3) the first tsunami wave (the highest in a CSZ M9
 379 scenario) arrives in the Barview area (due to being the most westward) at $t = 15 - 20$ mins,
 380 and starts to inundate to the west shoreline of the peninsula. The first wave arrives at the
 381 north side around $t = 30$ mins and the east side of Coos Bay around $t = 40$ mins. Most
 382 mortalities are observed on roads located in the west shoreline area, followed by the north
 383 and east sides.

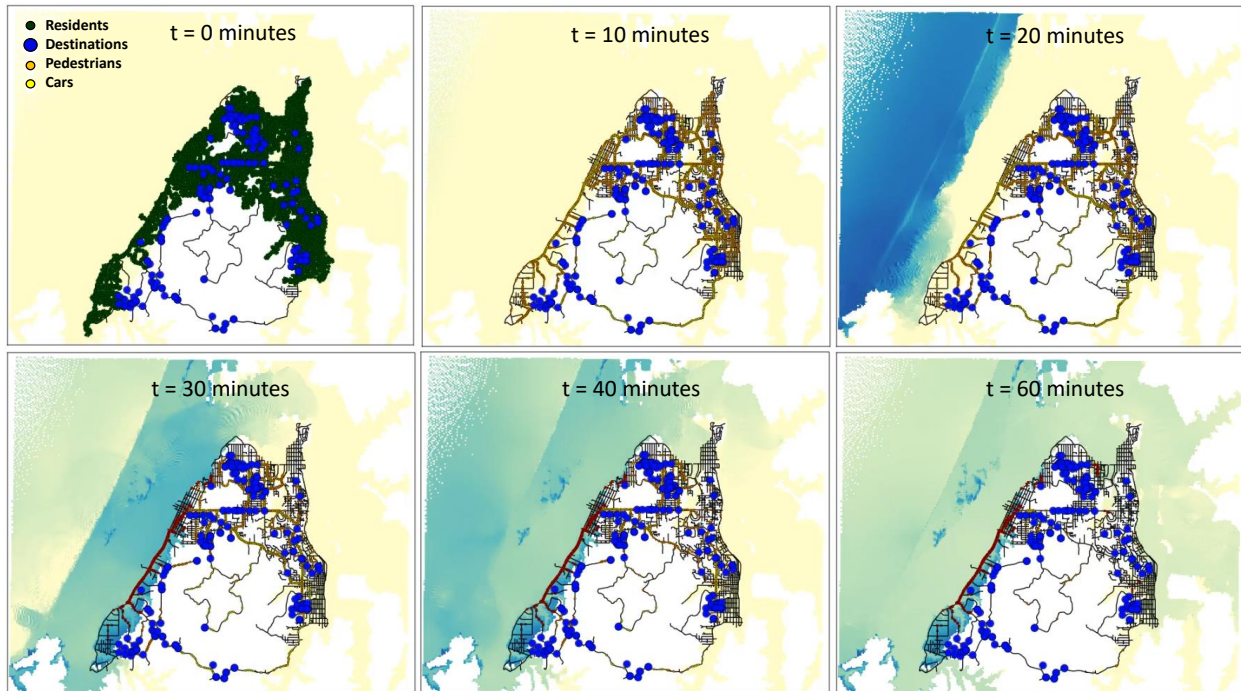


Figure 5: Model screenshot by time

384 Two scenarios are examined in this study. **Scenario 1** assumes that the tsunami is the only
 385 cause of disaster impacts in the community. Consequently, the road network functions at
 386 full capacity until it is inundated by the tsunami waves. Thus, Scenario 1 provides a baseline

387 for assessing the sensitivity of the modeling results to a plausible range of variation in the
388 values of the input variables. **Scenario 2** assumes that an M9 earthquake damages the
389 road network and impedes the evacuation process. According to this scenario, driving may
390 not be possible due to the heavy disruption of roads in large scale landslides, liquefaction,
391 lateral spreading, dropped power lines, debris, and traffic congestion. This assumption has
392 also been applied to previous studies of earthquake and tsunami preparedness in Washington
393 (WGS, 2021), Oregon (DOGAMI, 2020), and California (Cal OES, 2021).

394 *3.1. Scenario 1: variable testing with no network disruption*

395 Sensitivity analysis is applied to examine the impact of variation in each model variable on
396 the expected tsunami mortality rate. A Monte Carlo method is employed to capture the
397 probabilistic nature of the inputs and to create an interpretive mean.

398 *3.1.1. Evacuation Decision and Milling Time*

399 Figure 6 shows the sensitivity analysis for the impact of the evacuation participation rate and
400 milling time on mortality rate among the inundation zone population (100% measures only
401 the population live in the inundation zone). Consistent with previous studies (Mas et al.,
402 2013; Wang et al., 2016), these two variables have a significant impact on the estimated
403 mortality rate. The larger the percentage of people who decide to evacuate and the less time
404 people delay before departure, the lower the mortality rate will be. However, the impact of
405 milling time on mortality rate is complex, which yields two conclusions.

406 First, the change in the evacuation participation rate shows a smaller impact when milling
407 time increases. For example, there is no decrease in mortality rate when evacuation partici-
408 pation changes from 10% to 100% at 50 mins of milling time, whereas there is a 88%
409 mortality rate decrease when evacuation participation changes from 10% to 100% at 5 mins
410 of milling time. That is, the effect of decreasing milling time depends on the evacuation
411 participation rate.

412 Second, the curves that represent high evacuation participation rates in Figure 6 show an “S”
413 shape that indicates the rate of change in mortality is much larger in the middle range of the
414 x-axis from 15 minutes to 25 minutes. Given that the first tsunami wave will arrive on the
415 west side of the Coos Bay peninsula around 15 minutes after the earthquake, the mortality
416 rate will increase substantially as milling time increases past that threshold. Conversely,
417 when milling time is less than 5 minutes and 100% of people decide to evacuate, the curve
418 shows that the mortality rate is extremely low (less than 2%). Thus, the results indicate
419 that reducing the milling time is an important objective for tsunami preparedness programs
420 but it will be most effective when the evacuation participation rate is high.

421 This result confirms the policy of public authorities on the US west coast (WGS, 2021;
422 DOGAMI, 2020; Cal OES, 2021) to emphasize “Do Not Wait” in their tsunami educational
423 brochures and other outreach products to encourage people to depart as soon as possible
424 after earthquake shaking subsides. Although our simulation findings support this recommen-
425 dation, gaps remain in the response from local residents. Comparing the survey results of
426 the two variables from Coos Bay (gray areas) with the sensitivity analysis curves shows that
427 the mortality rate is fairly low if based on residents’ intended milling time, but it can still
428 be improved by further decreasing milling time and encouraging more people to evacuate.
429 The same holds true for Crescent City, CA (Chen et al., 2021).

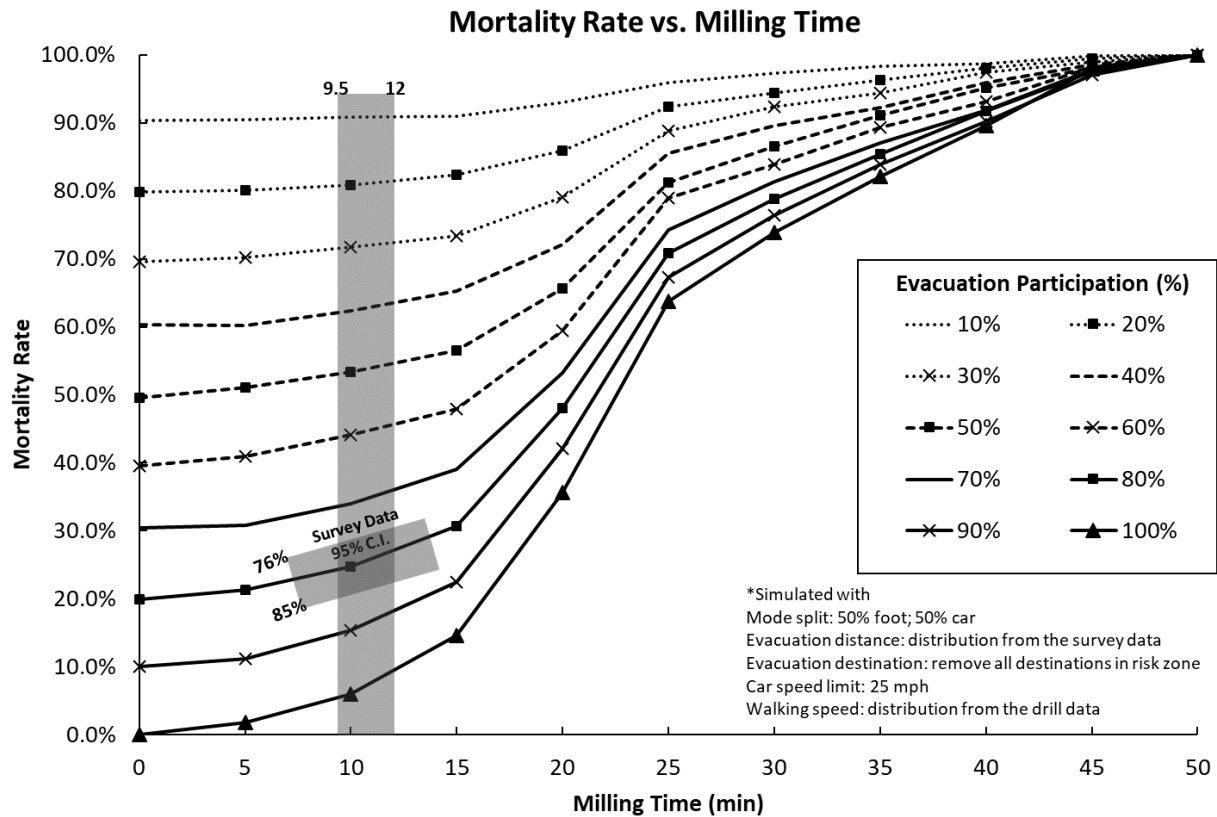


Figure 6: Estimated mortality rate of the inundation zone population as a function of milling time and evacuation participation

3.1.2. Mode Choice and Walking Speed

Coastal authorities in the CSZ advise evacuating by foot if possible, not only because of potential traffic congestion, but because the road network is likely to be so disrupted that driving may not be feasible to evacuate from a local tsunami. Of course, roads could be flooded by a distant tsunami for which no earthquake shaking could be felt. However, distant tsunamis such as those from the 1964 Alaska and 2011 Japanese tsunamis will take hours to reach the Oregon coast. Consequently, people will have the option of driving when distant tsunamis threaten. Thus, research is needed to examine authorities' recommendation to evacuate by foot and help emergency managers decide when to advise pedestrian evacuation instead of vehicular evacuation. This section analyzes the impact of mode choice and walking speed during evacuation from a local tsunami, and answers the question: Can walking beat driving? If so, in what situations?

Figure 7 shows how walking speed and mode choice influence tsunami mortality estimates. As walking speed increases beyond 1 m/s, the estimated mortality rate decreases as the walking percentage increases. Conversely, as walking speed decreases below 1 m/s, the estimated mortality rate decreases as fewer people choose to walk. This result indicates that if everyone can walk faster than 1 m/s, it is beneficial for more people to evacuate on foot. Given that 0.91 m/s is a slow walking speed and 1.22 m/s is a moderate walking speed threshold for unimpaired adults (Knoblauch et al., 1996; Langlois et al., 1997; Wood and Schmidlein,

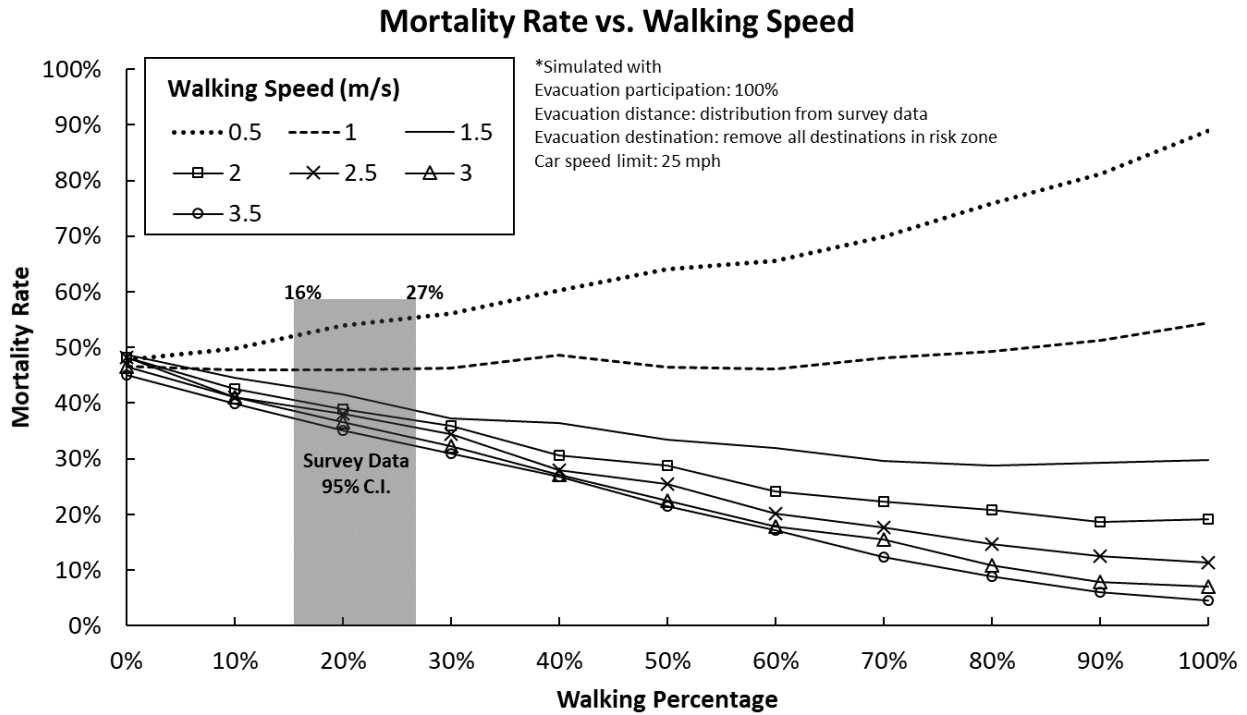


Figure 7: Mortality rate changes by mode choice and walking speed

449 2012; Fraser et al., 2014), it follows that evacuating on foot is better than evacuating by car
 450 if people can walk faster than the slow walking speed threshold. This finding also implies that
 451 if people who can walk faster than 1 m/s choose to walk, road network capacity can be saved
 452 for mobility impaired people so they can avoid traffic congestion during their evacuation.
 453 This is consistent with the finding that 30% evacuation by car and 70% evacuation by foot is
 454 the critical threshold for tsunami evacuation in Seaside (Mostafizi et al., 2019b). Similarly,
 455 vehicular traffic capacity can be saved for those 30% of the risk area population so they can
 456 reach safety in time. However, the question remains: Who should evacuate by car? Even
 457 though our finding suggests that most unimpaired people should walk to save traffic capacity
 458 for the vulnerable population, risk area residents may behave differently. The survey results
 459 show that only 21% of the respondents (95% C.I. 16%–27%) expect to evacuate by foot in
 460 Coos Bay (Chen et al., 2021), even though Oregon authorities encourage everyone to do so
 461 (DOGAMI, 2020). It is unclear whether this disparity is due to people not having received
 462 this recommendation or if they have received it and have chosen not to comply with it.
 463 It should be noted that the results shown in Figure 7 describe the overall picture of evacuation
 464 in Coos Bay, but the situation may be different for people living in unique areas that are
 465 a long distance from safety, so smaller-scale ABMS or BtW analyses are needed. However,
 466 given that the high ground spine in the middle of the Coos Bay peninsula provides a nearby
 467 evacuation destination, few people are likely to be in that situation.

468 3.1.3. Other Variables and Combinations of Variables

469 Many variables may vary during the evacuation and local authorities need to prioritize
 470 resources by deciding which variables or combinations of variables have the greatest impact

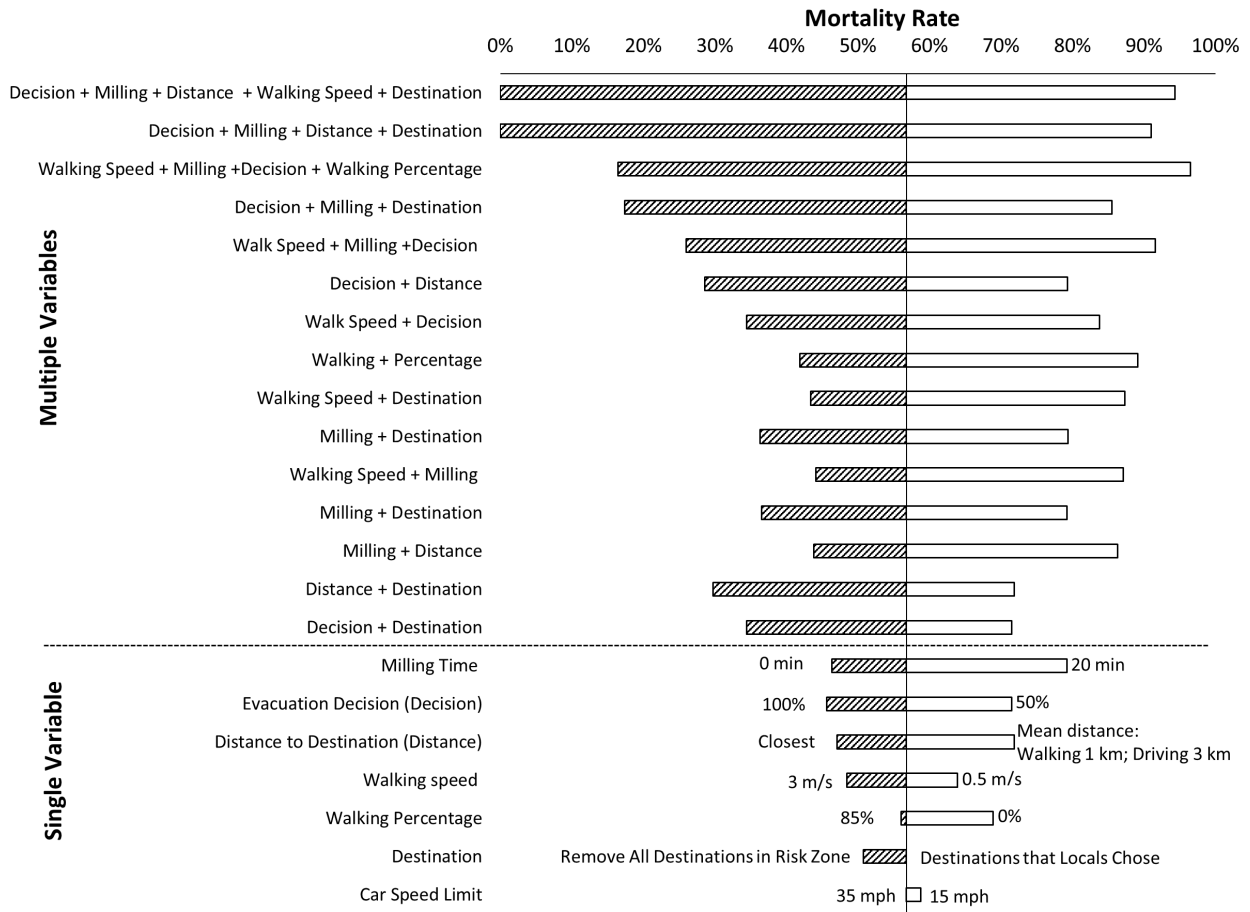


Figure 8: Impact range of model variables

471 on expected mortalities. Figure 8 shows the impact on mortality rate of variation in the
 472 plausible range of single and multiple variables. The estimated mortality rate for the Coos
 473 Bay inundation zone is just over 57% if all of the variables are at their most probable
 474 values (the vertical line in the center of the figure) and the bottom bar shows that there
 475 is almost no variation in mortality rate as car speed varies from its plausible lower bound
 476 (15 mph) to its plausible upper bound (35 mph), whereas it ranges from 45–85% if milling
 477 time ranges from 0–20 mins. However, the results show that variation in *Milling Time* and
 478 *Evacuation Decision* have the greatest impact on expected mortality when these variables
 479 are analyzed individually. This result is consistent with the discussion for Figures 6 and
 480 7 and previous simulation research (Mas et al., 2013; Mostafizi et al., 2019b). Variation
 481 in *Distance to Destination* also has a relatively large impact range. Specifically, the lowest
 482 mortality occurs when evacuees choose the closest destination and increases when they choose
 483 farther destinations. This is because agents tend to spend more time traveling on the roads
 484 within the inundation area when they choose farther destinations. This is especially true for
 485 residents living on the west coastal shoreline where the Cape Arago Highway stretches along
 486 the shoreline in the inundation zone as the only major road to connect this area to other
 487 regions in Coos Bay. When a tsunami strikes, some people who lack knowledge about the

488 inundation area and first wave arrival time may travel on this highway to seek safety farther
489 inland. We observed this “overshooting” behavior in the survey data from both Coos Bay
490 and Crescent City (Chen et al., 2021). The maximum car speed has the lowest impact (2% on
491 mortality rate) of all variables, which is consistent with findings from Mostafizi et al. (2019b)
492 showing the impact range of max car speed is about 2.5 percentage points from 15–35 mph.
493 This finding confirms that driving travel speed is not determined by the maximum speed one
494 can drive at any moment but, rather, by overall road capacity and traffic conditions, which
495 are well-described in traffic flow theory.

496 The upper panel in Figure 8 shows the impact range of simultaneously changing two or more
497 variables to their lowest plausible levels. Although *Decision + Distance* and *Walking Speed +*
498 *Decision* have the largest ranges of impact for any pair of variables, there is a similar impact
499 range for other pairs. However, the results show even greater reductions in mortality esti-
500 mates when more than two variables are at their lowest plausible levels. For example, when
501 optimizing evacuation participation, milling time, and removing destinations in inundation
502 zone, the estimated mortality rate shrinks to less than 20%. When optimizing evacuation
503 participation, milling time, and choosing closest destinations outside of the inundation zone
504 (the second to the top bar), the results show that almost all residents can be saved. More-
505 over, increasing walking speed from 1.3 m/s to 5 m/s in addition to four other factors (the
506 top bar) produces a similar result. This result indicates that even evacuees who walk slowly
507 are very likely to reach safety in time if they leave immediately for a destination outside of
508 the inundation zone by shortest route. Local authorities should emphasize this finding when
509 deciding what information to communicate in their tsunami preparedness programs.

510 3.2. Scenario 2: considering network disruption when only walking is available

511 This section analyzes how network disruptions impact tsunami mortalities when walking is
512 the only option due to road network disruption of the type described in Section 2.3.3. Three
513 scenarios are included in this analysis: 1) when areas with at least moderate landslide-
514 liquefaction susceptibility are disrupted; 2) when only areas with at least high landslide-
515 liquefaction susceptibility are disrupted; and 3) when there is no network disruption.

516 As Figure 9 indicates, there is a nonlinear decrease in estimated mortality as walking speed
517 increases for all three scenarios. That the slopes of the lines decrease as walking speed
518 increases indicates that the marginal effect of changing walking speed on estimated mortality
519 is larger in the lower part of the range. For example, an increase from 0.5 m/s (slow walk)
520 to 1 m/s (normal walk) would yield a 24 percentage point decrease in estimated mortality.
521 However, when areas of the road network with at least moderate susceptibility are disrupted,
522 the model shows an increase of 9 percentage points in estimated mortality for all walking
523 speeds in the 0.25–1.5 m/s range, compared with the results for no disruption. When only
524 areas with a high level of susceptibility are disrupted, there is only a slight decrease in
525 estimated mortality, compared with the results for moderate disruption. When walking speed
526 increases to 1.5 m/s (fast walk), the impact of network disruption is minimal and almost all
527 people can successfully evacuate. Previous research on Seaside (Wang et al., 2016) found a
528 similar decrease to the one shown in Figure 9. In their study, estimated mortality decreased
529 to zero when walking speed increased to 2 m/s when there was no disruption. This similarity
530 suggests that similar results would be found in communities whose inundation zones have
531 similarly ready access to high ground.

532 The results from the ABMS is consistent with the results from the BtW model established
 533 for Coos Bay (Gabel et al., 2019) with slight differences shown in Figure 9. The similarity
 534 between the two models is likely due to the similar input parameters. For example, the survey
 535 data from Coos Bay suggest a gamma distribution ($\alpha = 1.66$, $\beta = 6.49$) to model milling
 536 time with mean = 10.77 mins; this distribution is used in the ABMS to define agents' milling
 537 time, whereas the BtW model assumes a 10 min fixed milling time (Gabel et al., 2019). The
 538 slight differences between the two results are also due to the inputs of the two models: the
 539 parameters are stochastic in the ABMS but fixed in the BtW model, even though they have
 540 similar means. The resulting similarities provide convergent validation of the two models, so
 541 that jurisdictions can choose either one depending on the purpose of study. The two models
 542 should not be considered mutually exclusive; a mixed-method model could be applied to
 543 more accurately assess evacuation results (Wood and Schmidlein, 2012). However, the
 544 convergence is based on the assumption that the survey respondents have accurate estimates
 545 of the time it takes them to prepare to leave. This is probably the case for those who
 546 have “grab and go” kits but is less likely for those who do not. In particular, research on
 547 the *planning fallacy* suggests that the survey data are underestimates for some respondents
 548 (Buehler et al., 2010).

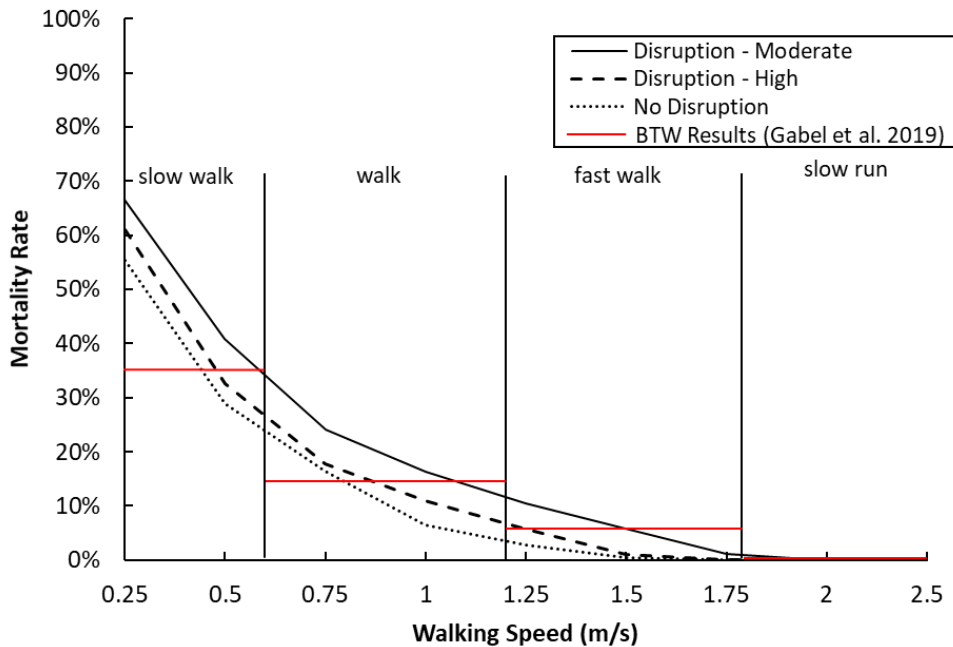


Figure 9: Network disruption impact: ABMS and BtW model result comparison

549 4. Conclusion

550 Although previous tsunami evacuation simulations have considered the natural environment,
 551 built environment, and social system in their models, many data inputs were arbitrary
 552 assumptions or adapted from studies of non-emergency situations, so the simulation results
 553 may not accurately reflect what would happen in a tsunami evacuation. The present study
 554 addressed this limitation by integrating behavioral data from community surveys into an

555 ABMS for a CSZ community. Four distinct contributions of this study are: 1) using the
556 PADM as a guide for collecting data on people’s expected evacuation behavior and the
557 integration of these data into the ABMS; 2) using empirical data from evacuation drills to
558 refine people’s evacuation walking speeds; 3) considering the impact of earthquake-caused
559 landslides and liquefaction on tsunami evacuation as a substantial aspect of the multi-hazard
560 situation; and 4) integrating the LCD component from the Wood and Schmidlein (2012)
561 BtW model – walking speed conservation by surface terrain and slope. By integrating
562 the natural environment, built environment, and social system, this model incorporates
563 substantial aspects of the real world into a multi-hazard ABMS. The simulation results
564 indicate that milling time and evacuation participation have significant non-linear impacts
565 on tsunami mortality estimates, which is consistent with Wang et al. (2016). The impact
566 of milling time on the mortality rate shows an “S” curve, so the impact of milling time
567 on estimated mortality varies the most when evacuation participation is highest. When
568 comparing which transportation mode people should take, the model result shows that more
569 people can reach safety in time when they choose to walk and are able to walk faster than 1
570 m/s (slow walk). These findings support an important point for tsunami education programs
571 in CSZ communities. Since the majority of Coos Bay respondents expected to evacuate by
572 car instead of on foot, local authorities need to emphasize the need for pedestrian evacuation
573 in their tsunami education programs.

574 This study also makes a significant contribution to understanding the impact of different
575 variables on tsunami mortality estimates. Evacuation success is more sensitive to walking
576 speed, milling time, evacuation participation, and choice of the closest safe location than
577 to other variables. Consistent with previous research, car speed has little impact on evac-
578 uation results. Further, this study also compared the sensitivities of different combinations
579 of variables. Tsunami mortality estimates are minimized when maximizing evacuation par-
580 ticipation, minimizing milling time, and choosing the closest safe destination outside of the
581 inundation zone. Furthermore, to validate this model, this study compared the ABMS re-
582 sults with the BtW model results from Gabel et al. (2019) for Coos Bay. Even though the
583 BtW model relies on a Geographical Information System rather than an ABMS, this study’s
584 preliminary comparison indicates a good match between results from the two models.

585 Finally, every study has limitations, as does this one. The agent decision and behavior is
586 based on survey data and drill data, rather than data from an actual tsunami evacuation, so
587 the results might not accurately predict the response to an actual tsunami. Future research
588 should investigate 1) the impact of more complex agent-agent interactions, such as leader-
589 follower behaviors and grouping behaviors (Chen et al., 2020), as well as car abandonment
590 (Wang et al., 2016); 2) the impact of building damage from earthquake before tsunami
591 (Gomez-Zapata et al., 2021); 3) authorities’ decision and warning dissemination processes for
592 distant tsunamis; and 4) validation of the model using data from actual tsunami evacuations.

593 **Code/Data availability**

594 The codes and data models used in this paper have been made available in open repositories.
595 Reader can also contact authors for details.

596 **Competing interests**

597 All authors declare that they have no conflict of interest.

598 **Author contribution**

599 Chen Chen: method and model development, analysis, and writing. Charles Koll: model
600 development and revising. Haizhong Wang and Michael Lindell: method development, anal-
601 ysis, and revising.

602 **Acknowledgement**

603 The authors would like to acknowledge the funding support from the National Science Foun-
604 dation through grants CMMI #1563618, #1826407, and #1826455. Any opinions, findings,
605 and conclusion or recommendations expressed in this research are those of the authors and
606 do not necessarily reflect the view of the funding agency. We are also thankful to Laura
607 Gabel and Jonathan Allan from DOGAMI for providing tsunami inundation model, as well
608 as their constructive suggestions and advises. This project was approved by the Oregon State
609 University Human Research Protection Program (HRPP) and Institutional Review Board
610 (IRB) and follows the regulations to protect participants, with project reference number
611 0489.

612 **References**

- 613 Bezanson, J., Karpinski, S., Shah, V. B., Edelman, A., Sep. 2012. Julia: A Fast Dynamic
614 Language for Technical Computing. arXiv:1209.5145 [cs].
615 URL <http://arxiv.org/abs/1209.5145>
- 616 Buehler, R., Peetz, J., Griffin, D., Jan. 2010. Finishing on time: When do predictions
617 influence completion times? *Organizational Behavior and Human Decision Processes*
618 111 (1), 23–32.
619 URL <https://linkinghub.elsevier.com/retrieve/pii/S0749597809000715>
- 620 Burns, W. J., Mickelson, K. A., Madin, I. P., 2016. Landslide Susceptibility Overview Map
621 of Oregon. Tech. Rep. REPORT O-16-02, Oregon Department of Geology and Mineral
622 Industries.
623 URL <https://www.oregongeology.org/pubs/ofr/p-0-16-02.htm>
- 624 Cal OES, 2021. How to Survive a Tsunami. Tech. rep., California Governor’s Office of
625 Emergency Services.
626 URL [https://www.conservation.ca.gov/cgs/Documents/Tsunami/How-to-Survive-](https://www.conservation.ca.gov/cgs/Documents/Tsunami/How-to-Survive-a-Tsunami.pdf)
627 [a-Tsunami.pdf](https://www.conservation.ca.gov/cgs/Documents/Tsunami/How-to-Survive-a-Tsunami.pdf)
- 628 Chen, C., Buylova, A., Chand, C., Wang, H., Cramer, L. A., Cox, D. T., Jun. 2020.
629 Households’ intended evacuation transportation behavior in response to earthquake and
630 tsunami hazard in a Cascadia Subduction Zone city. *Transportation Research Record*
631 2674 (7).
632 URL <http://journals.sagepub.com/doi/10.1177/0361198120920873>

- 633 Chen, C., Lindell, M. K., Wang, H., 2021. Tsunami preparedness and resilience in the
634 Cascadia Subduction Zone: A multistage model of expected evacuation decisions and
635 mode choice. *International Journal of Disaster Risk Reduction* 59, 102244.
636 URL <https://www.sciencedirect.com/science/article/pii/S2212420921002107>
- 637 Chen, X., Zhan, F. B., Jan. 2008. Agent-based modelling and simulation of urban
638 evacuation: relative effectiveness of simultaneous and staged evacuation strategies.
639 *Journal of the Operational Research Society* 59 (1), 25–33.
640 URL <https://www.tandfonline.com/doi/full/10.1057/palgrave.jors.2602321>
- 641 CLW, 2015. Geographic Features of the Coos Estuary and Lower Coos Watershed. Tech.
642 rep., The Communities, Lands & Waterways Data Source.
643 URL [http://www.partnershipforcoastalwatersheds.org/wordpress/wp-](http://www.partnershipforcoastalwatersheds.org/wordpress/wp-content/uploads/2015/08/FINAL-Geographic-Features-Data-Summary.pdf)
644 [content/uploads/2015/08/FINAL-Geographic-Features-Data-Summary.pdf](http://www.partnershipforcoastalwatersheds.org/wordpress/wp-content/uploads/2015/08/FINAL-Geographic-Features-Data-Summary.pdf)
- 645 Connor, D., 2005. Outreach assessment: How to implement an effective tsunami
646 preparedness outreach program. Tech. rep., State of Oregon Department of Geology and
647 Mineral Industries Open File Report OFR 0-05-10, Portland OR: Nature of the
648 Northwest Information Center.
649 URL https://www.oregongeology.org/pubs/ofr/0-05-10_onscreen.pdf
- 650 Cramer, L., Cox, D. T., Wang, H., 2018. Preparing for The Really Big One: The
651 Importance of Understanding the Local Culture of Resiliency. In: *Coastal Heritage and*
652 *Cultural Resilience*. Springer Press, New York, NY, pp. 243–264.
- 653 Dawson, R. J., Peppe, R., Wang, M., Oct. 2011. An agent-based model for risk-based flood
654 incident management. *Natural Hazards* 59 (1), 167–189.
655 URL <http://link.springer.com/10.1007/s11069-011-9745-4>
- 656 DOGAMI, 2020. Larger-Extent Evacuation Brochures. Tech. rep., State of Oregon
657 Department of Geology and Mineral Industries.
658 URL <https://www.oregongeology.org/tsuclearinghouse/pubs-evacbro.htm>
- 659 Franczyk, J. J., Burns, W. J., Calhoun, N. C., 2019. Statewide Landslide Information
660 Database for Oregon (SLIDO) Release 4.0. Tech. Rep. ORS 516.030, Oregon Department
661 of Geology and Mineral Industries.
662 URL <https://www.oregongeology.org/slido/data.htm>
- 663 Fraser, S. A., Wood, N. J., Johnston, D. M., Leonard, G. S., Greening, P. D., Rossetto, T.,
664 Nov. 2014. Variable population exposure and distributed travel speeds in least-cost
665 tsunami evacuation modelling. *Natural Hazards and Earth System Sciences* 14 (11),
666 2975–2991.
667 URL <https://nhess.copernicus.org/articles/14/2975/2014/>
- 668 Gabel, L. L. S., O'Brien, F. E., Bauer, J. M., Allan, J. C., 2019. Tsunami evacuation
669 analysis of communities surrounding the Coos Bay estuary: Building community
670 resilience on the Oregon coast. Tech. Rep. O-19-07, Oregon Department of Geology and

- 671 Mineral Industries.
672 URL <https://www.oregongeology.org/pubs/ofr/p-0-19-07.htm>
- 673 Gilbert, N., 2007. Agent-Based Models (Quantitative Applications in the Social Sciences).
674 SAGE Publication Ltd.
- 675 Gomez-Zapata, J. C., Brinckmann, N., Harig, S., Zafrir, R., Pittore, M., Cotton, F.,
676 Babeyko, A., Nov. 2021. Variable-resolution building exposure modelling for earthquake
677 and tsunami scenario-based risk assessment: an application case in Lima, Peru. *Natural*
678 *Hazards and Earth System Sciences* 21 (11), 3599–3628.
679 URL <https://nhess.copernicus.org/articles/21/3599/2021/>
- 680 Google, 2021. Google Earth.
681 URL <https://www.google.com/earth/versions/>
- 682 Gwynne, S., Galea, E. R., Owen, M., Lawrence, P. J., Filippidis, L., 1999. A review of the
683 methodologies used in evacuation modelling. *Fire and Materials* 23 (6), 383–388.
- 684 Hart, P., Nilsson, N., Raphael, B., 1968. A Formal Basis for the Heuristic Determination of
685 Minimum Cost Paths. *IEEE Transactions on Systems Science and Cybernetics* 4 (2),
686 100–107.
687 URL <http://ieeexplore.ieee.org/document/4082128/>
- 688 Karon, J., Yeh, H., 2011. Comprehensive Tsunami Simulator for Cannon Beach, Oregon.
689 Tech. rep., City of Cannon Beach.
690 URL [https://www.ci.cannon-beach.or.us/sites/default/files/](https://www.ci.cannon-beach.or.us/sites/default/files/fileattachments/demo_emergency_management/page/18691/cannon-beach-tsunami-final-report-may-2011.pdf)
691 [fileattachments/demo_emergency_management/page/18691/cannon-beach-](https://www.ci.cannon-beach.or.us/sites/default/files/fileattachments/demo_emergency_management/page/18691/cannon-beach-tsunami-final-report-may-2011.pdf)
692 [tsunami-final-report-may-2011.pdf](https://www.ci.cannon-beach.or.us/sites/default/files/fileattachments/demo_emergency_management/page/18691/cannon-beach-tsunami-final-report-may-2011.pdf)
- 693 Knoblauch, R. L., Pietrucha, M. T., Nitzburg, M., Jan. 1996. Field studies of pedestrian
694 walking speed and start-up time. *Transportation Research Record* 1538 (1), 27–38,
695 publisher: SAGE Publications Inc.
696 URL <https://doi.org/10.1177/0361198196153800104>
- 697 Langlois, J. A., Keyl, P. M., Guralnik, J. M., Foley, D. J., Marottoli, R. A., Wallace, R. B.,
698 Mar. 1997. Characteristics of older pedestrians who have difficulty crossing the street.
699 *American Journal of Public Health* 87 (3), 393–397.
700 URL <http://ajph.aphapublications.org/doi/10.2105/AJPH.87.3.393>
- 701 Lindell, M. K., 2018. Communicating imminent risk. In: Rodríguez H., Donner W., Trainor
702 J. (eds) *Handbooks of sociology and social research*, 2nd Edition. New York: Springer,
703 pp. 449–477.
- 704 Lindell, M. K., Murray-Tuite, P., Wolshon, B., Baker, E. J., 2019. Large-Scale Evacuation:
705 The Analysis, Modeling, and Management of Emergency Relocation from Hazardous
706 Areas. Routledge, p. 22.

- 707 Lindell, M. K., Perry, R. W., 1992. Behavioral foundations of community emergency
708 planning. Behavioral foundations of community emergency planning. Hemisphere
709 Publishing Corp, Washington, DC, US, pages: xi, 309.
- 710 Lindell, M. K., Perry, R. W., Apr. 2012. Theoretical modifications and additional evidence:
711 the protective action decision model. Risk Analysis 32 (4), 616–632.
712 URL <http://doi.wiley.com/10.1111/j.1539-6924.2011.01647.x>
- 713 Lindell, M. K., Prater, C. S., Mar. 2007. Critical Behavioral Assumptions in Evacuation
714 Time Estimate Analysis for Private Vehicles: Examples from Hurricane Research and
715 Planning. Journal of Urban Planning and Development 133 (1), 18–29.
716 URL [http://ascelibrary.org/doi/10.1061/%28ASCE%290733-
717 9488%282007%29133%3A1%2818%29](http://ascelibrary.org/doi/10.1061/%28ASCE%290733-9488%282007%29133%3A1%2818%29)
- 718 Lindell, M. K., Prater, C. S., Gregg, C. E., Apatu, E. J., Huang, S.-K., Wu, H. C., Jun.
719 2015. Households' immediate responses to the 2009 American Samoa earthquake and
720 tsunami. International Journal of Disaster Risk Reduction 12, 328–340.
721 URL <https://linkinghub.elsevier.com/retrieve/pii/S2212420915000266>
- 722 Madin, I. P., Burns, W. J., 2013. Ground motion, ground deformation, tsunami inundation,
723 coseismic subsidence, and damage potential maps for the 2012 Oregon Resilience Plan
724 for Cascadia Subduction Zone Earthquakes. Tech. Rep. REPORT O-13-06.
725 URL <https://www.oregongeology.org/pubs/ofr/p-0-13-06.htm>
- 726 Mas, E., Adriano, B., Koshimura, S., Mar. 2013. An integrated simulation of tsunami
727 hazard and human evacuation in La Punta, Peru. Journal of Disaster Research 8 (2),
728 285–295.
729 URL <https://www.fujipress.jp/jdr/dr/dsstr000800020285>
- 730 Mas, E., Suppasri, A., Imamura, F., Koshimura, S., 2012. Agent-based simulation of the
731 2011 Great East Japan Earthquake/Tsunami evacuation: An integrated model of
732 tsunami inundation and evacuation. Journal of Natural Disaster Science 34 (1), 41–57.
733 URL
734 https://www.jstage.jst.go.jp/article/jnds/34/1/34_41/_article/-char/ja/
- 735 Mori, N., Takahashi, T., Yasuda, T., Yanagisawa, H., Apr. 2011. Survey of 2011 Tohoku
736 earthquake tsunami inundation and run-up. Geophysical Research Letters 38 (7),
737 n/a–n/a.
738 URL <http://doi.wiley.com/10.1029/2011GL049210>
- 739 Mostafizi, A., Wang, H., Cox, D., Cramer, L. A., Dong, S., Sep. 2017. Agent-based tsunami
740 evacuation modeling of unplanned network disruptions for evidence-driven resource
741 allocation and retrofitting strategies. Natural Hazards 88 (3), 1347–1372.
742 URL <http://link.springer.com/10.1007/s11069-017-2927-y>
- 743 Mostafizi, A., Wang, H., Cox, D., Dong, S., Mar. 2019a. An agent-based vertical evacuation
744 model for a near-field tsunami: Choice behavior, logical shelter locations, and life safety.

745 International Journal of Disaster Risk Reduction 34, 467–479.
746 URL <https://linkinghub.elsevier.com/retrieve/pii/S221242091830918X>

747 Mostafizi, A., Wang, H., Dong, S., Nov. 2019b. Understanding the multimodal evacuation
748 behavior for a near-field tsunami. *Transportation Research Record* 2673 (11), 480–492.
749 URL <http://journals.sagepub.com/doi/10.1177/0361198119837511>

750 Nagarajan, M., Shaw, D., Albores, P., Aug. 2012. Disseminating a warning message to
751 evacuate: A simulation study of the behaviour of neighbours. *European Journal of*
752 *Operational Research* 220 (3), 810–819.
753 URL <https://linkinghub.elsevier.com/retrieve/pii/S0377221712001580>

754 Oregon Geospatial Enterprise Office, 2017. Oregon 10m Digital Elevation Model (DEM).
755 URL [https://spatialdata.oregonexplorer.info/geoportal/details?id=](https://spatialdata.oregonexplorer.info/geoportal/details?id=7a82c1be50504f56a9d49d13c7b4d9aa)
756 [7a82c1be50504f56a9d49d13c7b4d9aa](https://spatialdata.oregonexplorer.info/geoportal/details?id=7a82c1be50504f56a9d49d13c7b4d9aa)

757 OSM, 2021. OpenStreetMap.
758 URL <https://www.openstreetmap.org/>

759 Priest, G. R., Witter, R. C., Zhang, Y. J., Wang, K., Goldfinger, C., Stimely, L. L.,
760 English, J. T., Pickner, S. G., Hughes, K. L. B., Wille, T. E., Smith, R. L., 2013.
761 Tsunami inundation scenarios for Oregon. Tech. Rep. Open_file Report O-13-19, Oregon
762 Department of Geology and Mineral Industries.
763 URL <https://www.oregongeology.org/pubs/ofr/0-13-19.pdf>

764 Priest, G. R., Zhang, Y., Witter, R. C., Wang, K., Goldfinger, C., Stimely, L., Jun. 2014.
765 Tsunami impact to Washington and northern Oregon from segment ruptures on the
766 southern Cascadia Subduction Zone. *Natural Hazards* 72 (2), 849–870.
767 URL <http://link.springer.com/10.1007/s11069-014-1041-7>

768 Raskin, J., Wang, Y., Feb. 2017. Fifty-Year Resilience Strategies for Coastal Communities
769 at Risk for Tsunamis. *Natural Hazards Review* 18 (1), B4016003.
770 URL <http://ascelibrary.org/doi/10.1061/%28ASCE%29NH.1527-6996.0000220>

771 Sassa, S., Takagawa, T., Jan. 2019. Liquefied gravity flow-induced tsunami: first evidence
772 and comparison from the 2018 Indonesia Sulawesi earthquake and tsunami disasters.
773 *Landslides* 16 (1), 195–200.
774 URL <http://link.springer.com/10.1007/s10346-018-1114-x>

775 Schmidlein, M. C., Wood, N. J., Jan. 2015. Sensitivity of tsunami evacuation modeling to
776 direction and land cover assumptions. *Applied Geography* 56, 154–163.
777 URL <https://linkinghub.elsevier.com/retrieve/pii/S0143622814002690>

778 Soule, R. G., Goldman, R. F., May 1972. Terrain coefficients for energy cost prediction.
779 *Journal of Applied Physiology* 32 (5), 706–708.
780 URL <https://www.physiology.org/doi/10.1152/jappl.1972.32.5.706>

- 781 Tobler, W., 1993. Three Presentations on Geographical Analysis and Modeling: Non-
782 Isotropic Geographic Modeling; Speculations on the Geometry of Geography; and Global
783 Spatial Analysis (93-1). University of California at Santa Barbara: National Center for
784 Geographic Information and Analysis., 26.
785 URL <https://escholarship.org/uc/item/05r820mz>
- 786 Treiber, M., Hennecke, A., Helbing, D., Aug. 2000. Congested traffic states in empirical
787 observations and microscopic simulations. *Physical Review E* 62 (2), 1805–1824.
788 URL <https://link.aps.org/doi/10.1103/PhysRevE.62.1805>
- 789 United State Census Bureau, 2020. QuickFacts: United States; Crescent City city,
790 California; North Bend city, Oregon; Coos Bay city, Oregon. Tech. rep.
791 URL [https://www.census.gov/quickfacts/fact/table/US,](https://www.census.gov/quickfacts/fact/table/US,crescentcitycalifornia,northbendcityoregon,coosbaycityoregon/PST045219)
792 [crescentcitycalifornia,northbendcityoregon,coosbaycityoregon/PST045219](https://www.census.gov/quickfacts/fact/table/US,crescentcitycalifornia,northbendcityoregon,coosbaycityoregon/PST045219)
- 793 Wang, H., Mostafizi, A., Cramer, L. A., Cox, D., Park, H., Mar. 2016. An agent-based
794 model of a multimodal near-field tsunami evacuation: Decision-making and life safety.
795 *Transportation Research Part C: Emerging Technologies* 64, 86–100.
796 URL <https://linkinghub.elsevier.com/retrieve/pii/S0968090X15004106>
- 797 WGS, 2021. Tsunami Hazards in Washington State. Tech. rep., Washtington Geological
798 Survey, Washington State Department of Natural Resources.
799 URL https://www.dnr.wa.gov/publications/ger_tsunami_hazards_brochure.pdf
- 800 Witter, R. C., Zhang, Y., Wang, K., Priest, G. R., Goldfinger, C., Stimely, L. L., English,
801 J. T., Ferro, P. A., 2011. Simulating tsunami inundation at Bandon, Coos County,
802 Oregon, using hypothetical Cascadia and Alaska earthquake scenarios. Tech. Rep.
803 Special Paper 43, Oregon Department of Geology and Mineral Industries.
804 URL [https://www.oregongeology.org/tsuclearinghouse/resources/sp-43/SP-](https://www.oregongeology.org/tsuclearinghouse/resources/sp-43/SP-43_onscreen144dpi.pdf)
805 [43_onscreen144dpi.pdf](https://www.oregongeology.org/tsuclearinghouse/resources/sp-43/SP-43_onscreen144dpi.pdf)
- 806 Wood, M. M., Mileti, D. S., Bean, H., Liu, B. F., Sutton, J., Madden, S., Jun. 2018.
807 Milling and public warnings. *Environment and Behavior* 50 (5), 535–566.
808 URL <http://journals.sagepub.com/doi/10.1177/0013916517709561>
- 809 Wood, N. J., Jones, J., Spielman, S., Schmidlein, M. C., Apr. 2015. Community clusters of
810 tsunami vulnerability in the US Pacific Northwest. *Proceedings of the National Academy*
811 *of Sciences* 112 (17), 5354–5359.
812 URL <http://www.pnas.org/lookup/doi/10.1073/pnas.1420309112>
- 813 Wood, N. J., Schmidlein, M. C., Jun. 2012. Anisotropic path modeling to assess
814 pedestrian-evacuation potential from Cascadia-related tsunamis in the US Pacific
815 Northwest. *Natural Hazards* 62 (2), 275–300.
816 URL <http://link.springer.com/10.1007/s11069-011-9994-2>
- 817 Youd, T. L., Perkins, D. M., Apr. 1978. Mapping Liquefaction-Induced Ground Failure
818 Potential. *Journal of the Geotechnical Engineering Division* 104 (4), 433–446.
819 URL <http://ascelibrary.org/doi/10.1061/AJGEB6.0000612>